PAPER

Cationic micelles in deep eutectic solvents: effects of solvent composition†

Iva Manasi, [ID] [a] Stephen M. King [ID] [b] and Karen J. Edler [ID] *[c]

Deep eutectic solvents (DES) are mixtures of hydrogen bond donors and acceptors that form strongly hydrogen-bonded room temperature liquids. Changing the H-bonding components and their ratios can alter the physicochemical properties of deep eutectic solvents. Recent studies have shown *p*-toluenesulfonic acid (pTSA) forms room temperature liquids with choline chloride (ChCl) at different molar ratios: 1 : 1, 1 : 2 and 2 : 1 [Rodriguez Rodriguez *et al.*, *ACS Sustain. Chem. Eng.*, 2019, **7**(4), 3940]. They also showed that the composition affects the physical properties of these liquids and their ability to dissolve metal oxides. In this work we evaluate the solubility and self-assembly of cationic surfactants alkyltrimethyl ammonium bromides (CnTAB) in these pTSA/ChCl based liquids. CnTABs are insoluble in 1pTSA : 2ChCl, whereas in 1pTSA : 1ChCl and 2pTSA : 1ChCl they form micelles. We characterise CnTAB (n = 12, 14, 16) micelles using small angle neutron scattering and also look at interaction of water with the micelles. These studies help determine the interaction of DES components with the surfactant and the influence of varying pTSA and water ratios on these interactions. This provides potential for controlled surfactant templating and for tuning rheology modification in such systems.

1   Introduction

Deep eutectic solvents (DES) are molecular mixtures which share many features with ionic liquids (ILs) *e.g.* tunable physicochemical properties which makes them viable solvents that are more straightforward to prepare than typical ILs.[1,2] They enable self-assembly for a range of surfactants where the shape, size and morphology of micelles can be manipulated by altering the DES components and/ or their ratios. The interplay of factors such as solvent composition, water content, the hydrophobicity of solvent components and their degree of dissociation all play a role in surfactant self-assembly in these ionic mixtures, but are not

[a]Department of Chemistry, University of Bath, Claverton Down, Bath, BA2 7AX, UK. E-mail: im554@bath.ac.uk

[b]ISIS Neutron and Muon Source, Rutherford Appleton Laboratory, Didcot, OX11 0QX, UK

[c]Department of Chemistry, Centre for Analysis and Synthesis (CAS) Lund University, Lund, 221 00, Sweden. E-mail: karen.edler@chem.lu.se

† Electronic supplementary information (ESI) available. See DOI: **https://doi.org/10.1039/d4fd00045e**

yet well understood. The manipulation of micelle morphology is key to exploiting surfactants in applications from formulation of creams and gels for drug delivery[3–5] to templating of mesoporous materials.[6–8] Novel deep eutectic solvents (DES) are now being investigated as solvents for materials synthesis, reaction solvents and also as drug delivery systems since their components frequently include species which can enhance skin penetration. We are therefore investigating micelle formation and the key parameters to alter micelle morphology[8–17] in these complex ionic solvents.

Recently deep eutectic solvents formed from p-toluenesulfonic acid (pTSA) with choline chloride (ChCl) at different molar ratios were evaluated by Rodriguez Rodriguez *et al.*[18] comparing both their physical properties and ability to dissolve metal oxides. Other authors have used pTSA : ChCl mixtures at various molar ratios in applications ranging from the extraction of cellulose nanocrystals from biomass[19] or biofuel production[20] to cathode recycling of Li-ion batteries.[21] In water, pTSA is known to cause massive elongation in $C_{16}TA^+$ micellar systems, causing formation of highly viscous wormlike micelles.[22,23] The mechanism is proposed to be due to insertion of the amphiphilic anion into the micelle interface, altering the headgroup area, to promote micelle elongation. We have previously demonstrated that the presence of acidic species as DES components can, through interactions with the quaternary ammonium headgroups of C_nTA^+ surfactants, cause micelle elongation to some extent[11] and hydrotrope induced micellar growth for CTA^+ has been reported in choline chloride : glycerol DES using sodium salicylate.[14] In this work we therefore have investigated the effects of the DES component, pTSA, that can potentially have both electrostatic and hydrophobic interactions with cationic micelles, to determine whether insertion of the toluene group can also promote formation of wormlike micelles in these solutions. We have prepared these DES, and demonstrated that cationic alkyltrimethylammonium bromide surfactants can be dissolved in these solvents but only at some pTSA : ChCl molar ratios: 1 : 1 & 2 : 1. Here we therefore investigated the effect of combining these molecular interactions on micellization of C_nTAB micelles in pTSA : ChCl solvents at molar ratios of 1 : 1 and 2 : 1 without and with 3 moles of added water.

2 Methods and materials

2.1 Materials

p-Toluenesulfonic acid monohydrate ($CH_3C_6H_4SO_3H \cdot H_2O$; pTSA; 99%), choline chloride ($[(CH_3)_3NCH_2CH_2OH]Cl$; ChCl; $\geq$99%), dodecyl trimethylammonium bromide (DTAB, $\geq$99%), tetradecyl trimethylammonium bromide (TTAB, $\geq$99%) and hexadecyl trimethylammonium bromide (CTAB, $\geq$98%) were purchased from Sigma Aldrich, UK. Deuterated choline chloride-d9 ($[(CD_3)_3NCH_2CH_2OH]Cl$; d-ChCl; 99 at%, 98% D) and deuterated p-toluenesulfonic acid monohydrate-d7 ($CD_3C_6D_4SO_3H \cdot H_2O$; d-pTSA; 99 at%, 98% D) were purchased from Cambridge Isotope Laboratories. Isotopically labeled surfactants consisting of deuterated head and tail components (d34-DTAB, d38-TTAB, d42-CTAB) or with selective deuteration of the tail (d25-DTAB and d29-TTAB) were supplied by the STFC ISIS Deuteration Facility. Due to the hygroscopic nature of choline chloride, both h-ChCl and d-ChCl were dried under vacuum at 80 °C for at least 24 h

immediately prior to use in order to minimize water content in the resultant DES. All other chemicals were used as received without further purification.

2.2 Sample preparation

The pTSA : ChCl DES was prepared by combining the components in molar ratios of 1 : 1 or 2 : 1, as required. These mixtures were stirred at 60 °C until a clear, homogeneous liquid was obtained, which was subsequently sealed in a vial. The DES containing water were made by mixing pTSA : ChCl : water in the ratio 1 : 1 : 3 or 2 : 1 : 3 and then following the same procedure as above. Once formed, the mixtures are stable in the liquid state at room temperature. Depending on the isotopic contrast of the DES being produced protonated or deuterated pTSA, ChCl or H_2O/D_2O were used. The DES are labelled as HHH DES for h-pTSA : h-ChCl : H_2O, DDD DES for d-pTSA : d-ChCl : D_2O and HDD DES for h-pTSA : d-ChCl : D_2O.

Surfactant in DES solutions containing DTAB, TTAB and CTAB were prepared by mixing the required concentration of surfactant (2 wt%, 5 wt% or 10 wt%) in the DES at 50 °C until homogeneous mixtures were obtained.

2.3 Methods

The densities of the solvents were determined from a triplicate average of measurements on an Anton Paar DMA 4500 M at 25 °C. The molecular volumes were calculated from the molar mass and density and used to calculate the neutron scattering length density (SLD) for the DES. The water content of the DES was measured in triplicate using a Hanna Instruments HI903 Karl Fischer Volumetric Titrator, which measures the ppm of water in a certain weight of the sample, which is then converted to a wt%.

Flow curves for the DES and DES with added surfactants were measured using a TA Instruments HR-3 Discovery Hybrid Rheometer operating in a parallel plate geometry (50 mm SALS plate) and maintained at 50 °C using a Peltier control. The stress response of the samples was measured for an applied shear rate ranging from 0.1–500 s^{-1}. Viscosity of the samples was calculated from the shear stress vs. shear rate response.

Small-angle neutron scattering (SANS) measurements were carried out on the SANS2D[24] instrument at the ISIS Pulsed Neutron and Muon Source, UK (experiment number RB2010418).[25] Using sample-to-detector distances of 2.4 m or 4 m and neutrons with wavelengths 2–16.5 Å, a useable q-range of 0.008–0.72 $Å^{-1}$ was obtained. The neutron beam incident on the samples was collimated to 8 mm diameter. The samples were loaded into 1 mm path length rectangular quartz cuvettes (Hellma GmbH) and placed on a computer-controlled sample changer thermostatted by circulating fluid baths on the beamline. The measurements were performed at 50 °C, to ensure the solutions were above the Krafft temperature for all CnTAB in the DES. Data collection took 30–60 min per sample. Data reduction was performed according to the standard procedures at the instrument using the routines within the Mantid framework,[26] resulting in output converted to scattering intensity ($I(q)$, cm^{-1}) in absolute units on an absolute scale as a function of the scattering vector (q, $Å^{-1}$). Subtraction of the scattering from the pure solvents was performed afterwards using the NIST NCNR SANS reduction macros in Igor Pro[27] to account for the background contribution to each sample arising from incoherent scattering (primarily from 1H atoms).

Samples were prepared in different concentrations of CnTAB (2, 5 and 10 wt%) and different isotopic mixtures in the three DES (1pTSA : 1ChCl, 1pTSA : 1ChCl : 3W and 2pTSA : 1ChCl : 3W). Concentration series were measured for deuterated surfactant (d-Cn d-TAB or d-CnTAB) in protonated solvent (HHH DES; h-pTSA : h-ChCl : H_2O). To model the micelle structure, the 5 wt% CnTAB solutions in the three DES were measured at four contrasts: deuterated surfactant (d-Cn d-TAB or d-CnTAB) in protonated solvent (HHH DES; h-pTSA : h-ChCl : H_2O), protonated surfactant (h-Cn h-TAB or h-CnTAB) in deuterated solvent (DDD DES; d-pTSA : d-ChCl : D_2O), tail deuterated surfactant (d-Cn h-TAB) in protonated solvent (HHH DES; h-pTSA : h-ChCl : H_2O) and deuterated surfactant (d-Cn d-TAB or d-CnTAB) in partially deuterated solvent (HDD DES; h-pTSA : d-ChCl : D_2O).

2.4 Data analysis

The SANS data were analysed by co-fitting the various isotopic contrasts using standard spherical and ellipsoidal form factors and their core–shell variants in SasView.[28] The SLD calculations for the solvent and surfactants can be found in ESI Tables S3 and S4.† Details of the model fitting are provided in ESI Fig. S3 and Table S5.† Both spherical and ellipsoidal form factors can fit the data with low χ^2 values, but ultimately a spherical model was used to determine the micelle morphology as it gives more physically realistic parameters, and also the aspect ratio of the micelles as determined from the elliptical form factors is ≈ 1 and there is no improvement in the quality of the ellipsoidal fits (reduction in χ^2 values).

CnTAB surfactant self-assembly in DES has been shown to result in the formation of micelles with a core–shell density distribution, where the surfactant tails remain at the core of the aggregate surrounded by a shell of solvated headgroups.[9,11,15] Here, a uniform sphere model was initially used to find the overall shape and trends in size of the micelles. Subsequently, a core–shell model was used to determine the characteristics of the micelle cross-section. We considered either penetration of the solvent into just the head-group (core–shell spherical model) or also into a part of the tail region (core-2 shells spherical model) to capture the full details of the micelle structure in the DES, since there is some evidence of solvent penetration into the tail region of the micelles.

In the case of high concentration data, where inter-particle interactions were observed, the Percus–Yevick hard sphere structure factor[29] was used to account for the structure factor contribution to the scattering as employed in previous work on similar systems.[9,17] Details for the fitting models and procedure can be found in the ESI† (Section S4).

3 Results and discussion

Despite previous reports in the literature that pTSA : ChCl mixtures remain liquid at room temperature, we found that 2pTSA : 1ChCl and 1pTSA : 2ChCl froze when left on the benchtop overnight. This may be due to water content in the solvents – our measured water contents (see ESI Table S1†) were lower than those reported by other investigations on the same system. The 1 : 1 mixture solidified in the fridge at 5 °C, but remained liquid at 25 °C. The 2pTSA : 1ChCl DES became liquid on heating above 30 °C, and dissolved CnTAB surfactants at 60 °C, however the

Krafft temperature for these solutions was high, so the solutions were not reliably stable at 50 °C. For our SANS experiments therefore we have studied the solutions at 50 °C in the 1pTSA : 1ChCl mixture, and then compared the structures found in 1pTSA : 1ChCl : 3W and 2pTSA : 1ChCl : 3W, where the micellar solutions were stable.

3.1 Small angle neutron scattering studies

SANS was initially measured for all of the solvents alone, as backgrounds for the subsequent studies with surfactants. These data (see ESI Fig. S2†) indicate that these solvents are homogeneously structured, with no apparent clustering causing small angle scattering in the range measured (0.008–0.72 Å^{-1}). The contrasts where the choline cation and water are deuterated while pTSA is hydrogenated would be expected to have a signal in this range if significant clustering of the hydrophobic anion occurs. We also note that any pre-peak due to cation–anion ordering is at wider angles than measured in this experiment. Further studies of the structure of these solvents are currently underway.[30]

SANS was measured from solutions of d34-DTAB, d38-TTAB and d42-CTAB at 2, 5 and 10 wt% in each of the three HHH DES: 1pTSA : 1ChCl, 1pTSA : 1ChCl : 3W and 2pTSA : 1ChCl : 3W. The SANS data is shown in Fig. 1. These concentrations lie in the range 65 mM to 400 mM, depending on the surfactant and solvent (80 mM to 400 mM for DTAB, 70 mM to 360 mM for TTAB and 65 to 330 mM for CTAB; see ESI Table S2†), which is similar to the concentration range probed in previous studies of CnTAB surfactants in DES.[9,11,15,17] We do not have a reliable way to determine the critical micelle concentration (cmc) in this DES – the
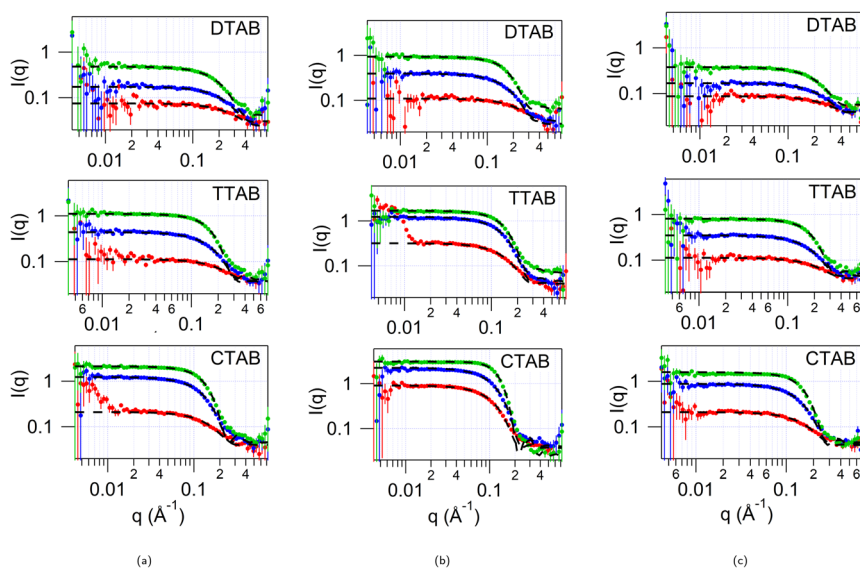

Fig. 1 SANS measured from 2 (red trace), 5 (blue trace) and 10 (green trace) wt% deuterated CnTAB surfactants in HHH DES: d34-DTAB (top panel), d38-TTAB (middle panel) and d42-CTAB (bottom panel). (a) CnTAB in 1pTSA : 1ChCl DES. (b) CnTAB in 1pTSA : 1ChCl : 3W DES. (c) CnTAB in 2pTSA : 1ChCl : 3W DES. The data is fitted to uniform spherical model (dashed lines).

hygroscopic nature and high viscosity makes surface tension measurements unreliable, the ionic strength is already high, preventing conductivity measurements, and fluorescence measurements were also unsuccessful, so previous studies were used to inform concentration studies. Confirmatory SAXS studies for CTAB show that at 1 wt% (*ca.* 32 mM) in 1pTSA : 1ChCl micellar scattering is observed however at 0.5 wt% (*ca.* 16 mM) we lose the micellar scattering signal suggesting that we may be close to the cmc so few if any micelles exist, or that we do not have enough contrast to measure them. For DTAB the same loss of micellar scattering is observed close to 1 wt% (*ca.* 40 mM). For comparison, in choline chloride : malonic acid (1 : 1) mixtures the cmc values were found to be 54 ± 6 mM for DTAB, 4.6 ± 0.5 mM for TTAB and 1.5 ± 0.3 mM for CTAB,[11] so the longer CTAB surfactant appears to be more soluble in the 1pTSA : 1ChCl mixture, while DTAB forms micelles at similar concentrations in both mixtures.

3.2 Effect of concentration

Previous studies have indicated that in choline chloride and acid based DES, micelle shape and size can be concentration dependant.[11] Here, in contrast, the shape of the micelle for all three surfactants, DTAB, TTAB and CTAB, is independent of the concentration, and a spherical model best describes the scattering data for all three concentrations. We note that in water, although CTAB forms more elongated micelles at higher concentrations, DTAB and TTAB are much less prone to elongate at high concentrations[31] even in the presence of salt,[32] while CTA^+ with chloride counterion has spherical micelles even at 1 M concentration.[31] In this DES there are multiple anionic species present, Br^-, Cl^- and pTS^- (likely to be dissociated due to the presence of water), which can compete to bind to the micelle surface, as well as with the quaternary ammonium moiety on the choline in the solvent. Using multiple contrasts, the SANS data were analysed to try to determine how the micelles might interact with these solvent components. As a starting point the SANS curves from various concentrations of DTAB, TTAB and CTAB in the three pTSA : ChCl DES, fitted to a uniform spherical model, with a hard-sphere structure factor to account for the inter-particle interactions at high concentrations, are shown in Fig. 1. The radius from the fits for the micelles at the different concentrations is given in ESI Table S6† and shown in Fig. 2.
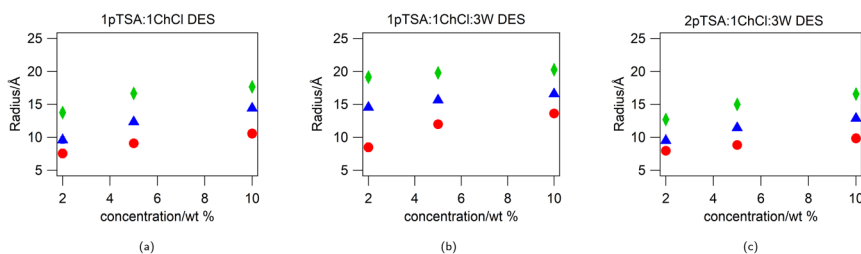

Fig. 2 Radius (from uniform spherical fits to the SANS data for d-CnTAB in HHH DES) *vs.* concentration for DTAB (red circles), TTAB (blue triangles) and CTAB (green diamonds) in the three DES: (a) 1pTSA : 1ChCl DES; (b) 1pTSA : 1ChCl : 3W DES; and (c) 2pTSA : 1ChCl : 3W DES. The error bars are smaller than the symbol size.

For all surfactants in all three DES, the effective spherical radius of the micelle increases as the concentration of the surfactant is increased. The biggest changes are observed for the surfactants in 1pTSA : 1ChCl, where the micelle radius increases with surfactant concentration by 3 Å for DTAB, 5 Å for TTAB and 4 Å for CTAB, and the smallest changes are observed for 1pTSA : 1ChCl : 3W, where the micelle radius increases by 5 Å for DTAB but shows little/no change for TTAB and CTAB over the concentration range studied.

A similar increase is observed for DTAB, CTAB and CTACl micelles in water, where the size of the micelle increases (as an increase in the aspect ratio of elliptical micelles) as the concentration of the surfactant is increased over a similar range.[31] This is in contrast to the observation for CnTAB micelles in ChCl : malonic acid DES, where the size of the micelle (radius and aspect ratio) remains unchanged for DTAB and TTAB but micelle length decreases (aspect ratio decreases while radius stays constant) for CTAB as the concentration of the surfactant increases. In other DES, containing neutral species such as urea or glycerol, rather than acids, the micelle size (both radius and aspect ratio) are independent of surfactant concentration.[9,15,17] In the case of micelles in water, the change in size of the micelles with concentration is attributed to the increase in charge neutralization of the headgroups due to an increase in the counterion condensation on the micelles with the concentration. This allows more surfactant molecules to pack into the self-assembled structures. Previous studies have also indicated that counterion condensation plays an important role in determining both the shape and size of micelles in DES[12,13] but trends opposite to that of water can be observed for ionic surfactants in DES, possibly due to the adsorption of bulky solvent molecules at the micelle interface.[11]

In the three DES studied here, both water and non-water solvent interactions with the micelle are important; we note that even the 1pTSA : 1ChCl DES contains water (1 mole) from the water of hydration of pTSA and therefore the variation of the size of micelle with concentration is dependant both on the surfactant investigated and the DES composition.

3.3 Effect of solvent constituents

Due to interparticle interactions between micelles at high concentrations (10 wt %), and low intensity and therefore poor signal to noise ratio at 2 wt%, 5 wt% was chosen as the optimum concentration to do multi-contrast studies to determine the detailed structure of the micelles in the three DES.

As we have already seen, in Fig. 1, the micelle size depends both on concentration and on the DES used, *e.g.* for d-DTAB in HHH DES at 5 wt% the fitted micelle radius is 9 Å in 1pTSA : 1ChCl, 12 Å in 1pTSA : 1ChCl : 3W and 9 Å in 2pTSA : 1ChCl : 3W. These values are small compared to the radius of a similar micelle in water (measured as *ca.* 8–17 Å in water depending on counterion[33]) which suggests that both counterion effects may play a role and also that solvent components may penetrate into the tail-filled core region, influencing the apparent size of the micelles.

To investigate this, contrast variation SANS was measured from 5 wt% d-CnTAB in HHH DES and h-CnTAB in DDD-DES and co-fitted to uniform spherical models. The SANS data along with the model fits and details of the parameters are shown in ESI Fig. S3 and Table S5.† The spherical micelle radius from

the fits for the three DES compositions is shown in Fig. 3a. For all three surfactants the micelles are largest in the 1pTSA : 1ChCl : 3W DES (radius is 12.5 Å for DTAB, 15.6 Å for TTAB and 19.4 Å for CTAB), implying that high water content favours bigger micelles and the micelles are smallest in the 2pTSA : 1ChCl DES (radius is 9.8 Å for DTAB, 12.0 Å for TTAB and 15.4 Å for CTAB), implying higher pTSA content favours smaller micelles. An effect similar to this is seen for DTAB in ChCl : malonic acid DES, where the aspect ratio of the micelles remains fairly constant but the equatorial radius increases on increasing the water content of the DES.[11] In the ChCl : malonic acid DES, this was attributed to change in solvent
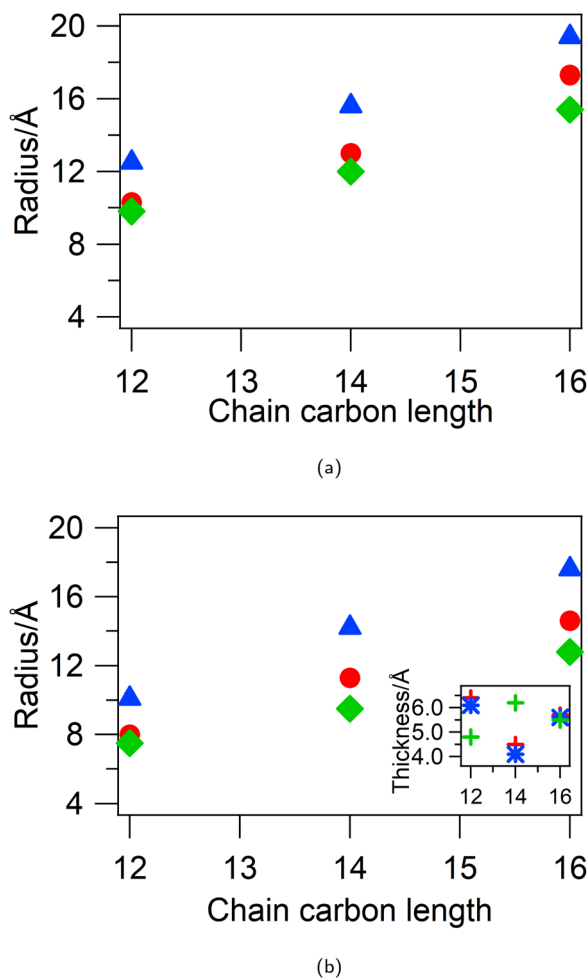

(a)

(b)

Fig. 3 Micelle radius from the fits to the SANS from 5 wt% CnTAB in the three DES: 1pTSA : 1ChCl (red circles), 1pTSA : 1ChCl : 3W (blue triangles), and 2pTSA : 1ChCl : 3W (green diamonds). (a) Radius from uniform spherical model cofitted to d-CnTAB in HHH DES and h-CnTAB in DDD DES; (b) core radius and shell thickness (inset) from core−shell spherical model cofitted to d-CnTAB in HHH DES, h-CnTAB in DDD DES and d-Cn h-TAB in HHH DES. The error bars are smaller than the symbol size.

penetration and polarity of the solvent which affects both micelle size and morphology.

There are two effects at play here: the counterion condensation from the ions (mainly Cl^-) and the effect of water and organic components, particularly pTSA, on the polarity of the solvent. For the three DES used in this study the molar ratio of pTSA : choline : water : chloride is 1 : 1 : 1 : 1 (all organics : water : Cl is 2 : 1 : 1) for 1pTSA : 1ChCl, 1 : 1 : 4 : 1 (all organics : water : Cl is 0.5 : 1 : 0.25) for 1pTSA : 1ChCl : 3W and 1 : 0.5 : 2.5 : 0.5 (all organics : water : Cl is 0.6 : 1 : 0.2) for 2pTSA : 1ChCl : 3W. The water ratio is therefore the highest in the 1pTSA : 1ChCl : 3W DES, followed by the 2pTSA : 1ChCl : 3W DES and finally the 1pTSA : 1ChCl DES. However, the 2pTSA : 1ChCl : 3W DES also has a large fraction of the non-polar pTSA, so on the balance of polar to non-polar components we would expect the 1pTSA : 1ChCl : 3W DES to be the most polar. This would mean that it is less energetically favorable for the surfactant molecules to leave the micelle and interact with the solvent. The presence of water would also impact counterion condensation/charge screening of the CTA^+ micelles. The two effects lead to larger spherical micelles, when compared to the other two solvents.

The 1pTSA : 1ChCl and 2pTSA : 1ChCl : 3W DES have a smaller difference in micelle size. The 1pTSA : 1ChCl DES is likely to be the least polar solvent overall and therefore more of the surfactant will dissolve in the DES than be found in micelles. This also results in a smaller micelle size, though not to the same extent as the 2pTSA : 1ChCl : 3W DES. The 2pTSA : 1ChCl : 3W, in addition to the non-polar pTSA reducing the polarity, also has the fewest Cl^- ions which can shield the quaternary ammonium headgroup of the surfactants. The reduced shielding means greater charge on the molecules reducing their packing. Together with the lower polarity, this leads to smallest spherical micelles.

3.4 Micellar structure

Berr *et al.*[33] have shown that CTA^+ micelles in water can be quite small (elliptical micelles with radii 8 Å and 13 Å for CTAOH and spherical micellar radius of 13 Å for CTACl) for counterions that exhibit inadequate screening, which prohibits close proximity of headgroups and limits the number of surfactant molecules that can pack into the micelle. Micelles with these counterions also do not show any elongation with increasing concentration even for C16 chain lengths, unlike that observed for CTAB and $CTANO_3$ in water. Our systems show similar behaviour, where due to charge screening effects and reduction in polarity of the solvent small, spherical micelles are formed for concentrations up to 10 wt% (*ca.* 330 mM) of CTAB. This may be also due in part to counterion exchange at the micelle surface of chloride and pTS anions from the solvent with the native bromide counterion of the surfactant. The bulky pTS anion could ion pair with the surfactant headgroups but prevent a reduction in headgroup area through steric bulk at the micelle surface, while chloride anions are less effective at screening than bromide. However, another possibility is the insertion of non-polar DES components (*e.g.* pTSA) into the micelle core, which leads to a change of neutron contrast and the micelle tail region appearing small.

In order to investigate this possibility, in addition to the above mentioned contrasts, we also measured d-Cn h-TAB in HHH DES and fully deuterated d-CnTAB in HDD DES. The first contrast was co-fitted with the d-CnTAB in HHH

DES and h-CnTAB in DDD DES to a core–shell spherical model with a core comprising the surfactant tails and a shell comprising head-groups with solvent penetration. The details of the fitting procedure are given in the ESI (Fig. S4†) and the parameters are summarised in Table S7.† The core–shell spherical micelle radius and the thicknesses from the fits for the three DES compositions are shown in Fig. 3b. The core-radius was found to be ∼2 Å smaller than that found in fits using the uniform spherical model, but following the same trend with the core-radius being smallest for 2pTSA : 1ChCl : 3W DES and largest for 1pTSA : 1ChCl : 3W DES. The shells have a thickness of 5.5 ± 1.0 Å, independent of the DES or surfactant, with a high DES volume fraction of 0.8 ± 0.1. The high volume fraction of DES in the shells masks any variations between different DES and may imply a layered solvent penetration *i.e.* two distinct regions of solvent penetration.

To account for any solvent penetration into the tail region of the micelles in addition to solvation of the headgroups, the data from the 4 measured contrasts (d-CnTAB in HHH DES, h-CnTAB in DDD DES, d-Cn-h-TAB in HHH DES and d-CnTAB in HDD DES) was therefore fitted to a core and two-shell model, with a core comprising only the tails of the surfactant, a shell taking into account some solvent penetration into the tail regions and a final shell comprising the head-groups along with the solvent components. The details of the fit constraints on the parameters are available in ESI Table S8.† The fits to DTAB in the three DES at all four contrasts are shown in Fig. 4 along with the fit parameters in Table 1. The data and fits for TTAB and CTAB are provided in ESI Fig. S5 and S6 and Tables S9 and S10,† respectively.

In these fits, we can see three distinct regions: an inner core comprising only the surfactant tails with a radius of 6.5–7.5 Å for DTAB, 7–8 Å for TTAB and 9–11 Å for CTAB, followed by a 4–7 Å shell (shell 1) and finally a 2–4 Å highly solvated (70–90% solvent) second shell (shell 2). It is difficult to get detailed volume fraction profiles of various components in the different shell regions due to the complexity in the system: shell 1 may comprise surfactant tails, along with the toluene ring of the pTSA and potentially the organic component of the choline cation; shell two can contain the surfactant head group along with some of the Cl$^-$ and Br$^-$ ions, the sulfonic acid part of the pTSA and water molecules. However, from the fitted value for the scattering length density (SLD) of the shell 1 region for the d-Cn d-TAB in HDD DES contrast (highlighted in italics in Table 1; SLD *ca.* 2.5×10^{-6}
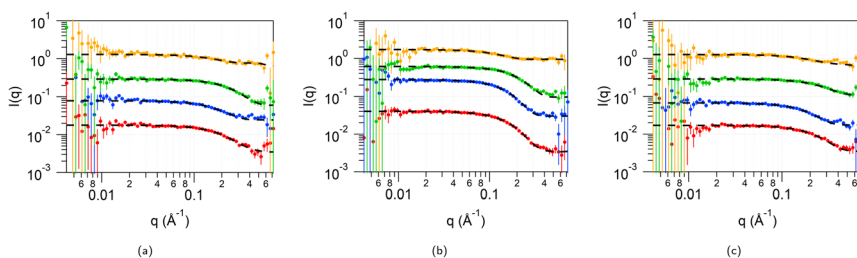

Fig. 4 SANS data from 5 wt% DTAB in the three DES at 4 contrasts: d-DTAB in HHH DES (red), h-DTAB in DDD DES (blue), d-D h-TAB in HHH DES (green) and d-DTAB in HDD DES (orange). (a) 5 wt% DTAB in 1pTSA : 1ChCl, (b) 5 wt% DTAB in 1pTSA : 1ChCl : 3W, and (c) 5 wt% DTAB in 2pTSA : 1ChCl : 3W. The data is fitted to core and two-shell model (dashed lines). The SANS patterns are offset along the *y*-axis for clarity.

Table 1 Fit parameters for core and two-shell model fitted to the SANS data from 5 wt% DTAB solutions in the three DES co-refined for the four contrasts: d-DTAB in HHH DES, h-DTAB in DDD, d-D h-TAB in HHH DES and d-DTAB in HDD DES

	Core-radius/Å	Shell 1 thickness/Å	Shell 2 thickness/Å	Shell 1 SLD/ $\times 10^{-6}$ Å^{-2}	Shell 2 SLD/ $\times 10^{-6}$ Å^{-2}
1pTSA : 1ChCl					
d-D d-TAB in HHH DES	6.6 ± 0.4	4.6 ± 1.1	3.2 ± 1.2	1.3 ± 0.2	1.2 ± 0.1
h-D h-TAB in DDD DES				3.5 ± 0.1	3.2 ± 0.1
d-D h-TAB in HHH DES				1.3 ± 0.2	0.9 ± 0.1
d-D d-TAB in HDD DES				*2.3 ± 0.3*	*3.4 ± 0.2*
1pTSA : 1ChCl : 3W					
d-D d-TAB in HHH DES	8 ± 0.8	6.1 ± 1.4	2.6 ± 1	1.4 ± 0.2	1.2 ± 0.4
h-D h-TAB in DDD DES				3.8 ± 0.4	4.2 ± 0.2
d-D h-TAB in HHH DES				1.4 ± 0.2	0.3 ± 0.2
d-D d-TAB in HDD DES				*3.2 ± 0.3*	*5.4 ± 1.1*
2pTSA : 1ChCl : 3W					
d-D d-TAB in HHH DES	6.3 ± 0.4	3.7 ± 1.1	3.8 ± 1	1.8 ± 0.5	1.1 ± 0.3
h-D h-TAB in DDD DES				3.2 ± 0.6	3.8 ± 0.2
d-D h-TAB in HHH DES				1.8 ± 0.5	0.9 ± 0.3
d-D d-TAB in HDD DES				*2.2 ± 0.3*	*3.3 ± 0.3*

Å^{-2}) and the fact that all other components apart from pTSA are deuterated: surfactant tail (SLD 6.4×10^{-6} Å^{-2}), surfactant head (SLD 7.1×10^{-6} Å^{-2}), choline chloride (SLD 5.2×10^{-6} Å^{-2}) and D$_2$O (SLD 6.4×10^{-6} Å^{-2}), we can unambiguously say that pTSA (SLD of the toluene ring of pTSA 1.1×10^{-6} Å^{-2}) is inserting into the tails forming the first shell region. The toluene of the pTSA is the most non-polar moiety in the solvent and therefore can indeed interact with the surfactant tails and insert into the core of the micelle. The size of this regions is 4–7 Å, which is consistent with the size of the toluene section of this molecule (~5 Å). The SLD of this region is not very dependant on the tail length of the surfactant (it stays constant between C12, C14 and is slightly higher for the C16 tails), but shows a small and consistent variation between the three DES with 1pTSA : 1ChCl : 3W showing the highest SLD (lowest content of the hydrogenated toluene from the pTSA) and 2pTSA : 1ChCl : 3W showing the lowest SLD (highest content of the hydrogenated toluene from the pTSA) across the three CnTABs that are investigated here. The micelle core radius added to the shell 1 thickness is the size of the tail region and was found to be 10–12 Å for DTAB, 12.5–15 Å for TTAB and

15.5–16.5 Å for the CTAB, still following the trend seen above of being the smallest for the 2pTSA : 1ChCl : 3W DES and largest for 1pTSA : 1ChCl : 3W DES. The micelle size in the three DES is still small, due to the charge screening and polarity effects in our solvent, but more comparable to the smaller micelles observed for some CTA$^+$ in water systems.[33] A schematic showing the proposed micelle cross-section is shown in Fig. 5.

3.5 Rheology

The viscosity *vs.* shear rate curves for the three DES, 1pTSA : 1ChCl, 1pTSA : 1ChCl : 3W and 2pTSA : 1ChCl : 3W, with 5 wt% DTAB, TTAB and CTAB are shown in Fig. 6. The three DES without surfactants exhibit Newtonian behaviour with no shear rate dependence of the viscosity over the shear range studied (0.1–500 s^{-1}) and an average viscosity of 0.125 ± 0.004 Pa s for 1pTSA : 1ChCl, which is consistent with the values obtained by Rodriguez Rodriguez *et al.*[18] The viscosity of 1pTSA : 1ChCl : 3W is 0.061 ± 0.006 Pa s and that of 2pTSA : 1ChCl : 3W is 0.064 ± 0.006 Pa s. The lower viscosity of the two DES with added water is consistent with the reduction in viscosity observed for DES upon addition of water.[16,34–36] The water content was found to be 5.2 wt% in the 1pTSA : 1ChCl, 16.8 wt% for 1pTSA : 1ChCl : 3W and 16.0 wt% for 2pTSA : 1ChCl : 3W. The similar water concentration could also explain the similar values for viscosity observed for the 1pTSA : 1ChCl : 3W and 2pTSA : 1ChCl : 3W DES.

The Newtonian behavior observed in the native DES is transformed into a pronounced shear-thinning behavior once CnTAB surfactants are added. The low shear viscosity of CnTAB solutions in 1pTSA : 1ChCl and 1pTSA : 1ChCl : 3W is almost 2 orders of magnitude higher than that of the native DES solution. For solutions CnTAB in 2pTSA : 1ChCl : 3W the low shear viscosity is almost an order of magnitude higher than that of the native DES. The 2pTSA : 1ChCl : 3W system has the smallest micelles out of the three DES studied here and therefore shows the least increase in viscosity whereas the 1pTSA : 1ChCl : 3W has the largest
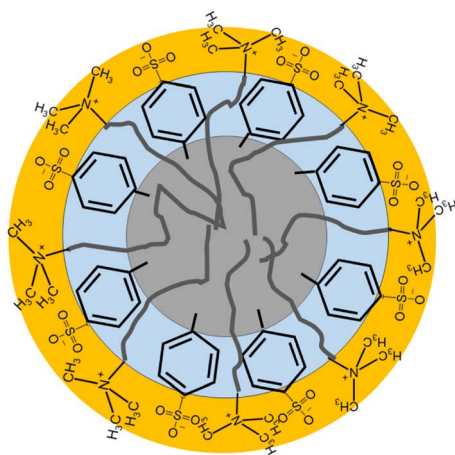

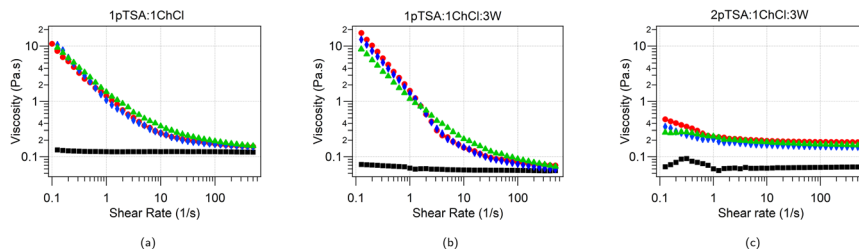Fig. 5 Micelle schematic for CnTAB micelles in the pTSA : ChCl DES based on the core and two-shell model.

Fig. 6 Viscosity *vs.* shear rate curves for the neat solvent (black squares) and solutions of 5 wt% DTAB (red circles), TTAB (blue diamonds) and CTAB (green triangles) in the three DES: (a) 1pTSA : 1ChCl DES; (b) 1pTSA : 1ChCl : 3W DES; and (c) 2pTSA : 1ChCl : 3W DES.

micelles and also shows the largest increase in viscosity when compared to the native DES. While typically shear thinning behaviour is not associated with spherical micelles, the shear forces could induce morphological/size changes in the micelles.[23,37] The initial low-shear increase in viscosity correlates with micelle size and the shear dependant lowering of viscosity could be associated with reduction in micelle size. The mechanism for this needs to be confirmed using a rheo-SANS experiment. We note that the distance between the largest micelles, even in the most concentrated solutions is still around 25 Å (*i.e.* for CTAB micelles in 1pTSA : 1ChCl : 3W DES where maximum micelle size is *ca.* 20 Å at 10 wt%; assuming all surfactant is in the micelles gives a highest possible volume fraction of 0.12, although from SANS fitting the volume fractions of the micelles are lower, around 0.08). The pTS$^-$ anion has a length of roughly 6 Å while the choline cation is 4.5 Å (see Fig. S1†) so between 2–3 cation–anion ion pairs would be needed to span the gap between micelles. Solvent binding to the micelle surface therefore seems unlikely to be directly responsible for the high viscosities measured in these solutions, although strong hydrogen bonding between solvent components and dissolved surfactant monomers, not in the micelles, may contribute.

For CTAB micelles in water, sodium toluenesulfonate is known to cause shear dependant flow behaviour, where shear thinning is observed at low shear rates followed by Newtonian plateau and finally leading to shear thickening at high shear rates.[38] This behaviour is attributed to the insertion of the pTSA moiety into the micelles, causing micellar elongation and the orientational and deformational effects of shear rate. Such behaviour is also observed for aqueous CTAB micellar solutions upon the addition of sodium salicylate, where rheo-optical methods show flow-induced stretching and alignment of micelles leading to shear-dependent flow behaviour. Here, however, the rheological studies on these solutions show that the micelles, although spherical in shape when the solution is at rest, can produce shear thinning behaviour indicating shear induced alignment, breakup/shrinkage or deformation of the micelles and potentially paving the way for these solutions to be used for rheology modification applications.

4 Conclusions

This study of cationic micelles in a deep eutectic solvent prepared from pTSA with choline chloride demonstrates the complex interplay of molecular interactions affecting self-assembly in these systems. Despite rheology data showing shear

dependant behaviour that is typically associated with non-spherical micelles our studies indicate that the scattering from the micelles can be adequately described by spherical models, even though the insertion of the pTSA species into the hydrophobic core of the micelles is also evident in this data. The SANS studies indicate that as the solvent mixture becomes more polar, containing more water, the micelle size increases, and in the less polar solvents smaller micelles form. Fitting of the SANS data for multiple contrasts indicates penetration of the pTSA component of the solvent into the micelles. The extent of pTSA penetration into the micelles is slightly lower in the largest micelles (and most polar solvent), but higher in the smallest micelles formed in the less polar solvents. pTSA carries a negative charge on the headgroup, and is a strong acid, so it is likely to be highly dissociated in these solutions, especially at the higher water contents. The dissociated pTSA will interact with the quaternary ammonium cations – both those in the surfactant and those in the choline likely forming ion pairs with both. In standard CTA^+ micelles in water at 303 K with different counterions the dissociation degree of Cl^- is 0.425, Br^- is 0.291 and pTS^- is 0.212 (ref. 39) so in an aqueous solution pTS might be assumed to out-compete the other two anions to bind to the micelle surface. However, this assumes these counterions are otherwise solvated by water. Here we have very little water, and a lower polarity solvent, in which pTS may be more soluble. From our results, the bulky nature of this ion, and its coordination to choline cations in the solvents appears to hinder strong shielding of the quaternary ammonium headgroups of the $CnTA^+$ surfactants, leading to the micelles remaining spherical under these conditions. In choline chloride : glycerol DES with added choline salicylate, similar penetration of the organic anion into the palisade region of CTAC micelles has been shown to occur, but in that case charge screening of the headgroups by this anion causes a reduction in headgroup area, facilitating formation of rod-like micelles at low water contents.[14] In that case addition of water also promoted formation of larger micelles, but *via* further elongation into wormlike micelles, rather than the larger spherical micelles observed in our case. Clearly the micelle geometries rely on a delicate balance of hydrophobic and electrostatic interactions, as well as steric factors in molecular packing into self-organised micelle structures. Deep eutectic solvents can support the self-organisation of amphiphilic molecules into nanoscale structures but resolving the competition between such interactions in these highly ionic mixtures to predict micellar morphologies remains challenging. Further experiments on solvent structures and their interactions with amphiphiles and small molecules such as water are needed, including under non-equilibrium conditions, to enable full use of the potential new toolbox of deep eutectic solvents.

Author contributions

K. J. E. and I. M. were involved in the conceptualisation of the experiments and writing the proposal for neutron beamtime access to carry out the SANS experiment. I. M. conducted the characterization studies and rheology experiments, made samples for SANS experiments, carried out the analysis and wrote the original draft for the paper. S. M. K. measured the SANS from the samples. K. J. E. and S. M. K. reviewed and edited the manuscript for the final draft.

Conflicts of interest

The authors declare no conflicts of interest.

Acknowledgements

Notes and references

1 Q. Zhang, K. De Oliveira Vigier, S. Royer and F. Jérôme, *Chem. Soc. Rev.*, 2012, **41**, 7108–7146.

2 D. O. Abranches and J. A. P. Coutinho, *Annu. Rev. Chem. Biomol. Eng.*, 2023, **14**, 141–163.

3 A. Banerjee, K. Ibsen, Y. Iwao, M. Zakrewsky and S. Mitragotri, *Adv. Healthcare Mater.*, 2017, **6**, 1601411.

4 M. Sakuragi, S. Tsutsumi and K. Kusakabe, *Langmuir*, 2018, **34**, 12635–12641.

5 D. J. G. P. van Osch, J. van Spronsen, A. C. C. Esteves, R. Tuinier and M. Vis, *Phys. Chem. Chem. Phys.*, 2020, **22**, 2181–2187.

6 X. Li, J. Choi, W.-S. Ahn and K. H. Row, *Crit. Rev. Anal. Chem.*, 2018, **48**, 73–85.

7 L. Hu, Z. Yan, J. Zhang, X. Peng, X. Mo, A. Wang and L. Chen, *J. Mater. Sci.*, 2019, **54**, 11009–11023.

8 I. Manasi, M. R. Andalibi, R. Castaing, L. Torrente-Murciano and K. J. Edler, *J. Mater. Chem. A*, 2022, **10**, 18422–18430.

9 A. Sanchez-Fernandez, T. Arnold, A. J. Jackson, S. L. Fussell, R. K. Heenan, R. A. Campbell and K. J. Edler, *Phys. Chem. Chem. Phys.*, 2016, **18**, 33240–33249.

10 A. Sanchez-Fernandez, K. J. Edler, T. Arnold, R. K. Heenan, L. Porcar, N. J. Terrill, A. E. Terry and A. J. Jackson, *Phys. Chem. Chem. Phys.*, 2016, **18**, 14063–14073.

11 A. Sanchez-Fernandez, O. S. Hammond, A. J. Jackson, T. Arnold, J. Doutch and K. J. Edler, *Langmuir*, 2017, **33**, 14304–14314.

12 A. Sanchez-Fernandez, O. S. Hammond, K. J. Edler, T. Arnold, J. Doutch, R. M. Dalgliesh, P. Li, K. Ma and A. J. Jackson, *Phys. Chem. Chem. Phys.*, 2018, **20**, 13952–13961.

13 A. Sanchez-Fernandez, A. J. Jackson, S. F. Prévost, J. J. Doutch and K. J. Edler, *J. Am. Chem. Soc.*, 2021, **143**, 14158–14168.

14 A. Sanchez-Fernandez, A. E. Leung, E. G. Kelley and A. J. Jackson, *J. Colloid Interface Sci.*, 2021, **581**, 292–298.

15 I. Manasi, M. R. Andalibi, R. S. Atri, J. Hooton, S. M. King and K. J. Edler, *J. Chem. Phys.*, 2021, **155**, 084902.

16 I. Manasi, S. J. Bryant, O. S. Hammond and K. J. Edler, *Eutectic Solvents and Stress in Plants*, Academic Press, 2021, vol. 97, pp. 41–68.

17 R. S. Atri, A. Sanchez-Fernandez, O. S. Hammond, I. Manasi, J. Doutch, J. P. Tellam and K. J. Edler, *J. Phys. Chem. B*, 2020, **124**, 6004–6014.

18 N. Rodriguez Rodriguez, L. Machiels and K. Binnemans, *ACS Sustainable Chem. Eng.*, 2019, **7**, 3940–3948.

19 M. A. Mariño, M. G. Paredes, N. Martinez, D. Millan, R. A. Tapia, D. Ruiz, M. Isaacs and P. Pavez, *Front. Chem.*, 2023, **11**, DOI: 10.3389/ fchem.2023.1233889.

20 A. Hayyan, M. A. Hashim, M. Hayyan, F. S. Mjalli and I. M. AlNashef, *J. Cleaner Prod.*, 2014, **65**, 246–251.

21 M. J. Roldán-Ruiz, M. L. Ferrer, M. C. Gutiérrez and F. d. Monte, *ACS Sustainable Chem. Eng.*, 2020, **8**, 5437–5445.

22 V. Patel, N. Dharaiya, D. Ray, V. K. Aswal and P. Bahadur, *Colloids Surf., A*, 2014, **455**, 67–75.

23 M. Takeda, T. Kusano, T. Matsunaga, H. Endo, M. Shibayama and T. Shikata, *Langmuir*, 2011, **27**, 1731–1738.

24 R. K. Heenan, S. E. Rogers, D. Turner, A. E. Terry, J. Treadgold and S. M. King, *Neutron News*, 2011, **22**, 19–21.

25 I. Manasi, K. J. Edler and S. M. King, *Tailoring micelle shape via solvent interactions in deep eutectic solvents-RB2010418*, 2020, DOI: 10.5286/ ISIS.E.RB2010418.

26 O. Arnold, J. Bilheux, J. Borreguero, A. Buts, S. Campbell, L. Chapon, M. Doucet, N. Draper, R. Ferraz Leal, M. Gigg, V. Lynch, A. Markvardsen, D. Mikkelson, R. Mikkelson, R. Miller, K. Palmen, P. Parker, G. Passos, T. Perring, P. Peterson, S. Ren, M. Reuter, A. Savici, J. Taylor, R. Taylor, R. Tolchenov, W. Zhou and J. Zikovsky, *Nucl. Instrum. Methods Phys. Res.*, 2014, **764**, 156–166.

27 S. R. Kline, *J. Appl. Crystallogr.*, 2006, **39**, 895–900.

28 SasView for Small Angle Scattering Analysis, https://www.sasview.org/.

29 J. K. Percus and G. J. Yevick, *Phys. Rev.*, 1958, **110**, 1–13.

30 I. Manasi, D. T. Bowron, E. K. Bathke and K. J. Edler, in preparation.

31 V. Aswal and P. Goyal, *Chem. Phys. Lett.*, 2003, **368**, 59–65.

32 V. Aswal and P. Goyal, *Chem. Phys. Lett.*, 2002, **364**, 44–50.

33 S. Berr, R. R. M. Jones and J. S. J. Johnson, *J. Phys. Chem.*, 1992, **96**, 5611–5614.

34 Y. T. Dai, G. J. Witkamp, R. Verpoorte and Y. H. Choi, *Food Chem.*, 2015, **187**, 14–19.

35 D. Shah and F. S. Mjalli, *Phys. Chem. Chem. Phys.*, 2014, **16**, 23900–23907.

36 C. Ma, A. Laaksonen, C. Liu, X. Lu and X. Ji, *Chem. Soc. Rev.*, 2018, **47**, 8685–8720.

37 H. Gochman-Hecht and H. Bianco-Peled, *J. Colloid Interface Sci.*, 2005, **288**, 230–237.

38 V. Hartmann and R. Cressely, *Colloid Polym. Sci.*, 1998, **276**, 169–175.

39 J. Mata, D. Varade and P. Bahadur, *Thermochim. Acta*, 2005, **428**, 147–155.